WCTE 2014 Quebec City Canada August 10-14
World Conference on Timber Engineering

NONLINEAR DYNAMIC ANALYSES OF NOVEL TIMBER-STEEL HYBRID SYSTEM

Michael Fairhurst[1], Xiaoyue Zhang[2], Thomas Tannert[3]

ABSTRACT: Although the benefits of using timber in mid- and high-rise construction are undisputed, there are perceived shortcomings with respect to the ductility needed to provide seismic resistance and a corresponding lack of appropriate design guidance. Overcoming these perceived shortcomings will allow timber, and its wood product derivatives, to further expand into the multi-storey construction sector, also in the context of hybrid structures that integrate different materials. The "Finding the Forest Through the Trees" (FFTT) system is a new hybrid system for high rise structures which combines the advantages of timber and steel as building materials. This paper presents research utilizing finite element models to capture the seismic response of the FFTT system and help developing design guidance. From the results presented herein, it appears that the FFTT system can meet the design performance requirements required for seismic loading: inter-storey drifts were lower than required and local plastic deformations were within a reasonable range for life safety performance.

KEYWORDS: FFTT System, Finite Element Models, Seismic Response, Nonlinear Dynamic Analyses

1 INTRODUCTION

The innovative hybrid system "Finding the Forest Through the Trees" (FFTT) is a proposed structural system for mid- and high-rise buildings [1]. The system utilizes engineered timber products to resist gravity and lateral loads with interconnecting steel members to provide the necessary ductility for seismic demands. The system reaps the light-weight, strength, stiffness, and environmental benefits of engineered timber, and exploits the ability of steel to dissipate energy and provide a ductile failure mechanism. Four different options for lateral force resisting systems (LFRS) are proposed for heights up to 30 stories; Options 1 and 4 are exemplarily shown in Figure 1 [1]. For a novel hybrid system, such as the FFTT, to gain recognition, experimental data must be gathered and supported by computational modelling and analysis to predict its structural performance. This paper presents nonlinear dynamic analyses utilizing finite element (FE) models to capture the seismic response of the FFTT system.

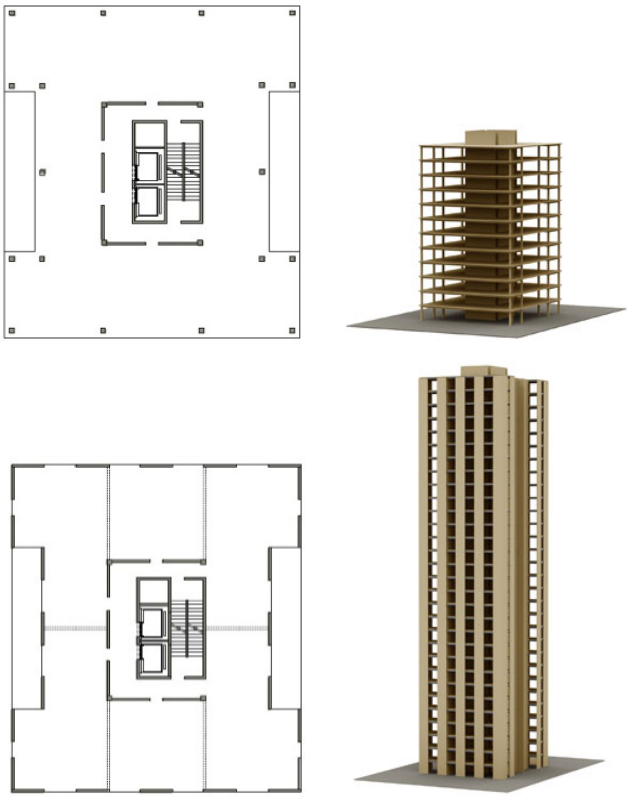

Figure 1: *FFTT system: Options 1 (top) and 4 (bottom) [1]*

[1] Michael Fairhurst, Research Assistant, Civil Engineering, UBC Vancouver, Canada, Email: fairhurstmike@gmail.com

[2] Xiaoyue Zhang, Research Assistant, Wood Science, UBC Vancouver, Canada, Email: xyzhang1211@gmail.com

[3] Thomas Tannert, Assistant Professor, Wood Science and Civil Engineering, UBC Vancouver, Canada, Email: thomas.tannert@ubc.ca (corresponding author)

2 NONLINEAR DYNAMIC ANALYSES

2.1 MODEL DEVELOPMENT

2.1.1 Software Platforms

The FFTT system was numerically modelled using SAP2000 [2] and OpenSees [3], an open source, object orientated software developed for earthquake engineering simulations. Preliminary analyses using SAP models (Figure 2) showed that the dynamic properties of the system were insensitive to whether or not the slabs were explicitly modelled with shell elements or simply captured through multi-point diaphragm constraints at each storey height. Thus, rigid diaphragm constraints were implemented in the OpenSees models to reduce modelling complexity and analysis time. The models represent both the dynamic elastic and inelastic behaviour of the structures. A typical storey of an Option 1 model is illustrated in Figure 3.

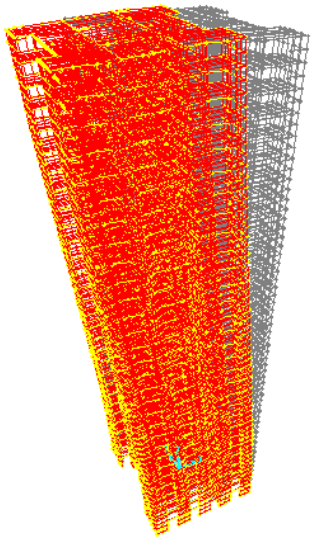

Figure 2: *First mode of a 30 storey example model*

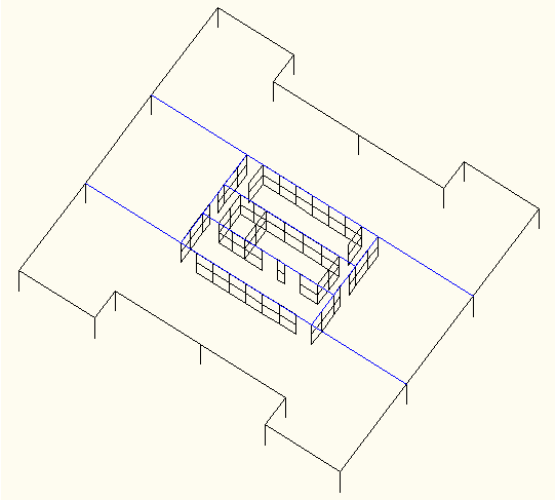

Figure 3: *FE model for typical storey of FFTT Option 1*

2.1.2 Timber Members

Accurate nonlinear modelling of any structure or material is a difficult task, even more so when dealing with an anisotropic material as timber. Timber when loaded in tension or shear is a brittle material, with failure occurring suddenly and almost without warning. To avoid sudden failure, timber structures are typically designed to fail in their connections, which are usually made using steel to provide a ductile failure mechanism and large amount of energy dissipation. The FFTT system considered in this study follows a similar design philosophy, in which steel beams that connect the main timber components are designed to yield before the timber members can fracture or crush. Consequentially, it is reasonable to model the timber components as purely elastic, as long as the complete nonlinear behaviour of the connections and the steel members are accurately captured.

The anisotropic properties of timber are considered by assigning different stiffness longitudinal and perpendicular to the grain. An elastic orthotropic material model which exists in the OpenSees platform is utilized to model shell elements that represent timber shear walls. Stiffness modifiers for the orthogonal directions were based on composite theory (also called K-Method) [4,5]. Beams and columns are simply modelled as elastic beam-column members.

The member sections are summarized in Table 1.

Table 1: *Structural member specifications*

Member	Material	Section
Glulam Beam	D. Fir 16c-E	264x484mm
Glulam Column	D. Fir 20f-EX	418x418mm
Steel Beam	Grade 350W	W250x33
CLT Wall	D. Fir	204mm (6 layers)
	or	274mm (8 layers)

The CLT floors, which act as rigid diaphragms were not explicitly modelled. The connections between the glulam perimeter frame members were included and modelled with nonlinear rotational springs based on glulam beam-column connection test results from Buchanen and Fairweather [6]. Since the maximum feasible length of a CLT panel is about 12m [1], to construct a CLT wall greater than four stories requires the connection of more than one CLT wall panel. These connections add flexibility to the wall and possibly yield due to higher mode effects producing large moments over the height of the structure. To account for this effect, axial springs were modelled along the shell nodes between adjacent shells at every fourth storey in each model. The springs allow the panels to rock in plane and potentially allow for yielding over the height of the wall. These springs were calibrated to CLT connection tests conducted by Popovski et al. [7] as shown in Figure 4.

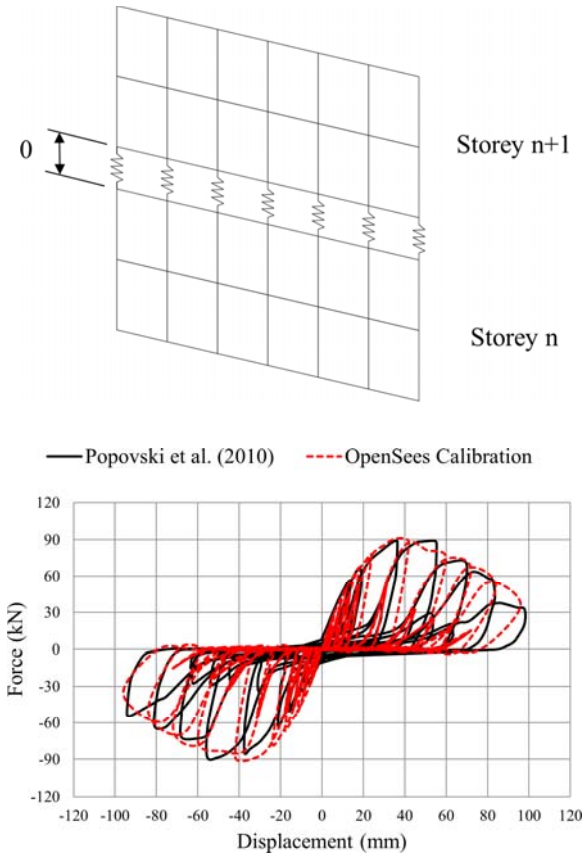

Figure 4: *(a) Wall model and (b) spring calibration*

The same member properties were used in all models; the thicker CLT wall panels (8 layers) were only used in the taller (20+ storey) models. All material properties were based on values from the appropriate Canadian design manuals [8,9].

Material properties for the CLT wall panels were based on local manufacturer's data [10], values proposed by Blass and Görlacher [11], and relationships as observed by Stürzenbecher et al. [12] as summarized in Table 2. E_0 and G_0 refer to the elastic and shear moduli parallel to the grain of the timber laminations, respectively. E_{90} and G_{90} refer to the elastic properties perpendicular to the grain of the timber. These properties are independent of the radial or tangential direction of the grain of the laminations.

Table 2: *CLT wall anisotropic material properties*

E_0	9500 MPa	E_{90}	500 MPa
G_0	700 MPa	G_{90}	50 MPa

2.1.3 STEEL MEMBERS

In the FFTT system, steel beams connect the timber wall elements and control the failure mechanism of the structure. Therefore, it is quintessential to the accuracy of the models to capture the yielding, hardening, and degradation properties of steel-timber connections.

One approach would be to model the beams as force- or displacement-based nonlinear elements by which curvature is obtained through integration over the section and element length. However, this is computationally intensive and would only capture the steel non-linear behaviour rather than the interaction between the steel and timber as each material undergoes plastic deformation (yielding and crushing). A simpler approach is to model the members as elastic, and to include a rotational spring near the end of the member, which is modelled to account for the inelastic properties of the entire connection including steel beam and timber panel. This approach can yield highly accurate results, while requiring a fraction of the computation time.

The hinges were calibrated to test results performed at the University of British Columbia (UBC) by Bhat [13]. Both monotonic and cyclic tests were performed on a variety of connections build by embedding steel beams into CLT panels as shown in Figure 5. In the tests, the beams were noted to yield before the timber began to crush. Due to this, the yielding moment and initial stiffness of the rotational springs were assigned according to the elastic section properties of the steel beam member. The nonlinear properties of the spring elements would capture both the steel yielding and subsequent timber crushing. The result moment-rotation relationship of a hinge calibrated to one of the test results is illustrated in Figure 6.

Figure 5: *Steel beam to CLT panel embedment [8]*

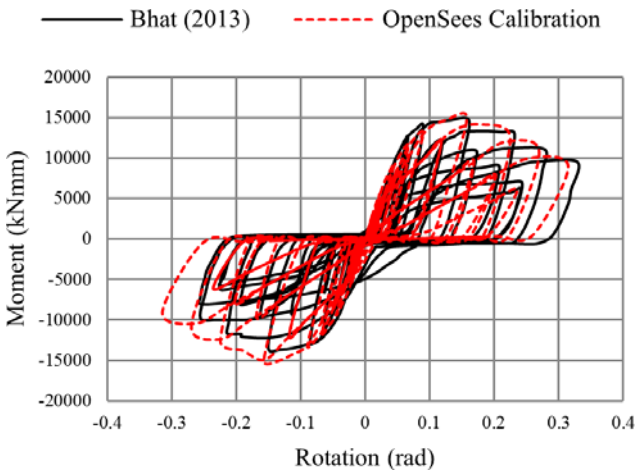

Figure 6: *With OpenSees calibrated test results on embedded HSS profile*

Since the resulting beam subassembly, comprising of a nonlinear hinge and elastic beam element, is essentially a model of two springs in series, the combined flexibility of the two elements would produce a model that is more flexible than an equivalent elastic beam member. To account for this, the elastic beam and nonlinear spring stiffness properties were modified by the method outlined by Ibarra and Krawinkler [14] so that the resulting hinge and elastic beam-column subassembly used in the FE models have the appropriate stiffness of an equivalent elastic member.

2.1.4 Boundary Conditions

The shear walls were modelled as pinned at the base with axial springs to simulate yielding and plastification of the supports. The pins were required to allow the desired failure mechanism (strong column-weak beam) to form, as shown in Figure 7; while the springs added stiffness against wall rocking yet could yield to prevent crushing stresses from developing in the CLT wall.

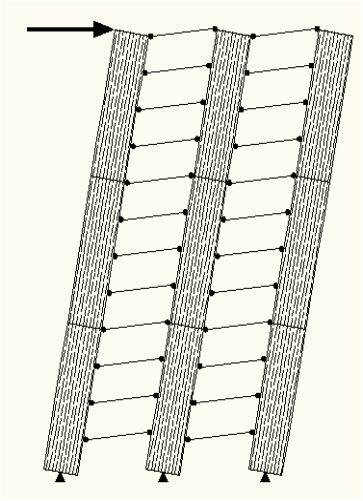

Figure 7: *FFTT system failure mechanism*

2.1.5 Mass and Weight

The structural members were designed for the gravity loads as summarized in Table 3 as well as earthquake (equivalent static force) and wind lateral loads with load combinations as specified in the National Building Code of Canada (NBCC 2010) [15] based on an $R_D R_O$ of 3 [1, 16]. Mass was assigned to the models in the two horizontal directions based on the weights specified in Table 3.

Table 3: *Design gravity loads [1]*

Load	Floors	Roof
Dead	4.0 kPa + perimeter walls	3.0 kPa
Live	1.9 kPa	1.8 kPa
Snow	-	1.8 kPa
Rain	-	0.2 kPa

2.1.6 Damping

Damping was applied as Rayleigh damping with a range of 4.4 to 6.6% of critical damping in the range of two thirds to three times the natural frequency (ω_1) of the models. This was accomplished by considering the method proposed by Hall [17], and is illustrated in Figure 8. The range used for the frequency was to cover to frequency range of response of the structures. Two thirds of ω_1 was chosen as a lower bound to estimate the frequency increase of the structure due to nonlinear softening; while $3\omega_1$ was to account for the effects of the second mode of vibration (in a building the behaves like a shear-beam the second frequency is approximately 3 times the first).

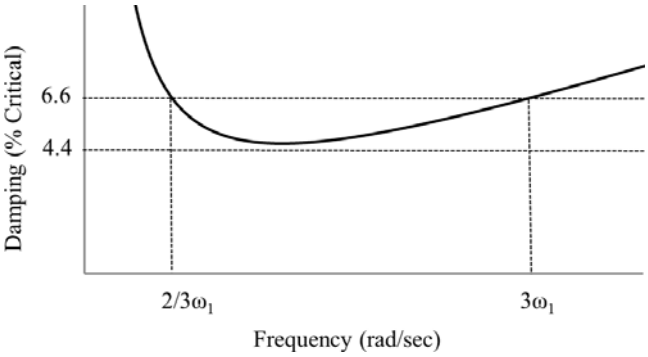

Figure 8: *Rayleigh damping frequency function*

2.2 GROUND MOTIONS

Ten bi-directional ground motions were selected from the FEMA P695 [18] far-field motion set, as listed in Table 4. The motions were chosen to resemble the hazard level at the proposed building location: Vancouver, BC. The 2% in 50 year (2475 year return period) 5% damped acceleration spectrum for Vancouver was selected as the design hazard level. The geometric mean (geomean) of each of the ten selected ground motions is shown in Figure 9, along with the average geomean and scaled average geomean. The ground motions were linearly scaled to match the design spectrum in the period range of the analysed structure.

Table 4: *Ground motion list*

Name	Recording Station
Northridge	Beverly Hills – Mulholland
Northridge	Canyon Country – WLC
Duzce, Turkey	Bolu
Hector Mine	Hector
Imperial Valley	Delta
Kocaeli, Turkey	Duzce
Landers	Yermo Fire Station
Loma Prieta	Gilroy Array #3
Superstition Hills	Poe Road (temp)
Chi-Chi, Taiwan	CHY101

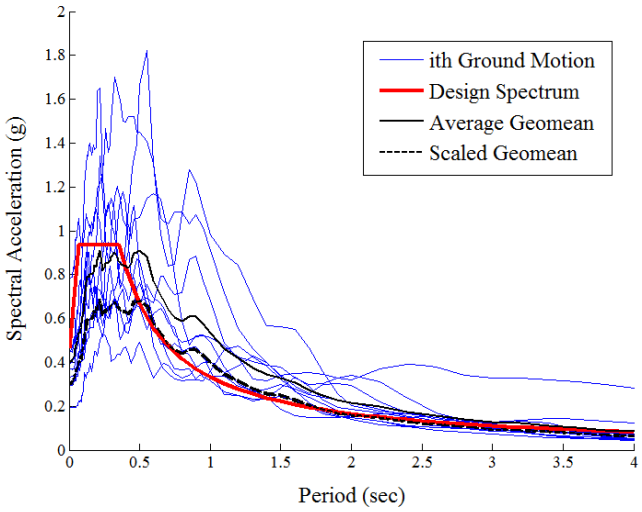

Figure 9: *Ground motion spectra and scaling example*

2.3 ANALYSIS

For each considered model and bi-directional ground motion, two analyses were run, one for each of the two main ground motion orientations (orientation of the primary component of the motion). The ground motions were always applied parallel to the primary axes of the structure. Then, for each scenario (a particular height of a particular building plan option subjected to a particular ground motion) the results were taken as the maximum of the two ground motion orientations. Figure 10 presents the displacement results of a 30 storey model subjected to the Chi-Chi, Taiwan ground motion orientated in both directions. The orientation which produces the higher response is taken as the result for that scenario (solid line).

For performance-based design of structures, building codes typically specify that mean response values may be used for design if seven or more ground motions are used in the analysis [15, 19, 20]. Since this study considered 10 unique motions, it is reasonable to base performance on the mean structural response from the 10 motions.

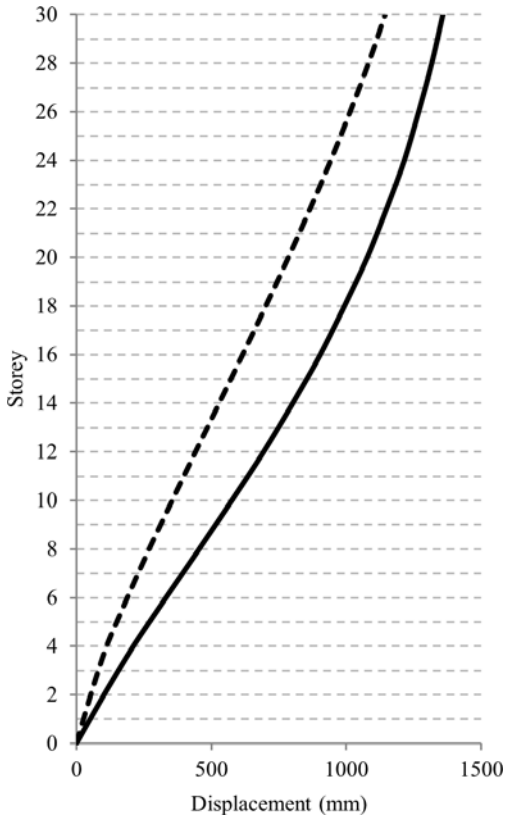

Figure 10: *Example 30 storey model displacement*

2.4 RESULTS

The stress state in each component was recorded during each analysis, not to determine the performance, but to ensure that all timber members did not reach their ultimate strength. This was to make sure that the elastic modelling assumptions used for the timber members were valid. This assumption held true throughout all of the analyses.

The following sections summarize the results of the suites of analyses based on predefined performance criteria. In total, 39 models of various heights and plan options were analysed in over 800 nonlinear dynamic time history analysis cases.

2.4.1 Inter-storey Drifts

The differential movement between adjacent floors, called interstorey drift, was selected as the main predictor of seismic performance for this study. Interstorey drift is calculated as the difference in deflection between adjacent stories, divided by the storey height, and is a main indicator of damage in most structural and non-structural components [21, 22].

The mean interstorey drift for each model of each of the four options is illustrated in Figure 11. The mean interstorey drift is calculated as the mean of the maximum responses observed from each of the ten ground motions.

An acceptable interstorey drift limit of 2.5% is proposed for this type of structure [1, 15, 16]. All of the models easily met this criterion. However this large limit may not be appropriate for this type of structure – since drift should be limited in the gravity resisting system to prevent unwanted failure in these timber members. To determine a stricter and more appropriate limit, the tests used to calibrate the connections in the gravity system [6] were considered. These tests comprised cyclic loading of a glulam beam-column assembly connected with steel brackets. In the specific test used for calibration for this study, a yielding rotation in the connection yielding a 1% storey drift was observed. Combining this with the elastic drift limit of the glulam member yields a total failure drift just over 1.1%. This value is much lower than the previously proposed 2.5% and should adequately ensure unwanted failure in the glulam gravity system. Figure 11 shows that all the models met this more stringent limit.

It may be noted that the interstorey drift tends to decrease with the height of the building, meaning that as the structures become taller, they become be less governed by earthquake load, in part due to their flexibility.

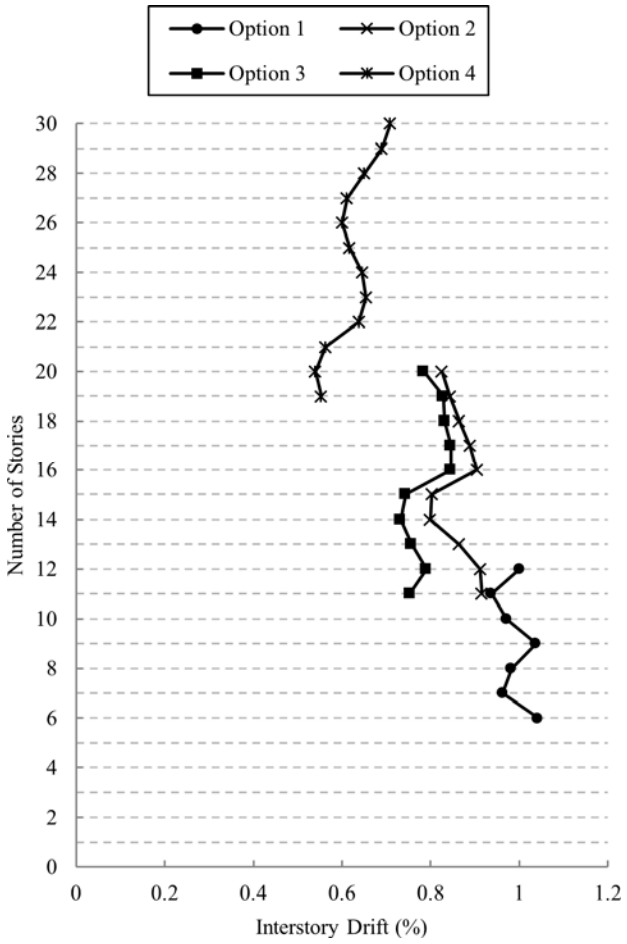

Figure 11: *Inter-storey drifts*

2.4.2 Roof Drift

Roof drift does not necessarily predict damage in a structure; however it is correlated to the performance of the structure and is included here as it may be useful to compare the seismic behaviour of the models.

The mean roof drift based on building height is presented in Figure 12. Once again it can be noted that drifts tend to decrease as the building height increases.

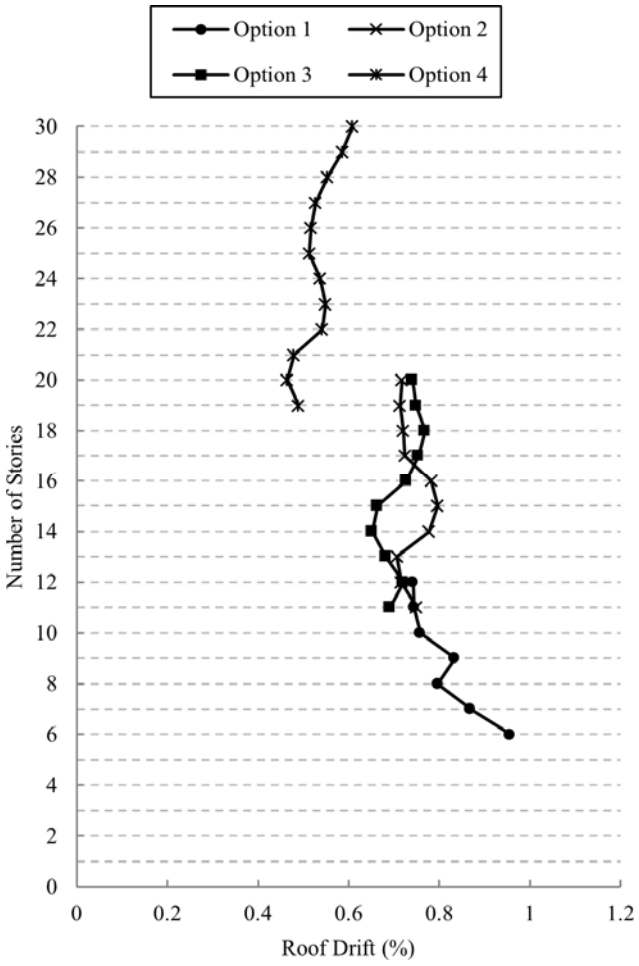

Figure 12: *Roof drifts*

2.4.3 PLASTIC ROTATIONS

Another predictor of damage in a structure is the inelastic rotation of its elements [23]. For this study the plastic rotation was recorded in the steel beams in order to determine the extent of localized damage in these elements.

To determine appropriate acceptance criteria, ASCE/SEI 41-06 [23] methodology was considered. For deformation controlled steel beam element, ASCE/SEI 41-06 typically defines life safety performance criteria as having a maximum plastic rotation less than or equal to the plastic rotation at which strength degradation begins.

The mean steel beam plastic rotations normalized by their life safety plastic rotation for each plan option are illustrated in Figure 13. All of the building heights had maximum plastic rotations equal to or less than 50% of their life safety values, which is acceptable.

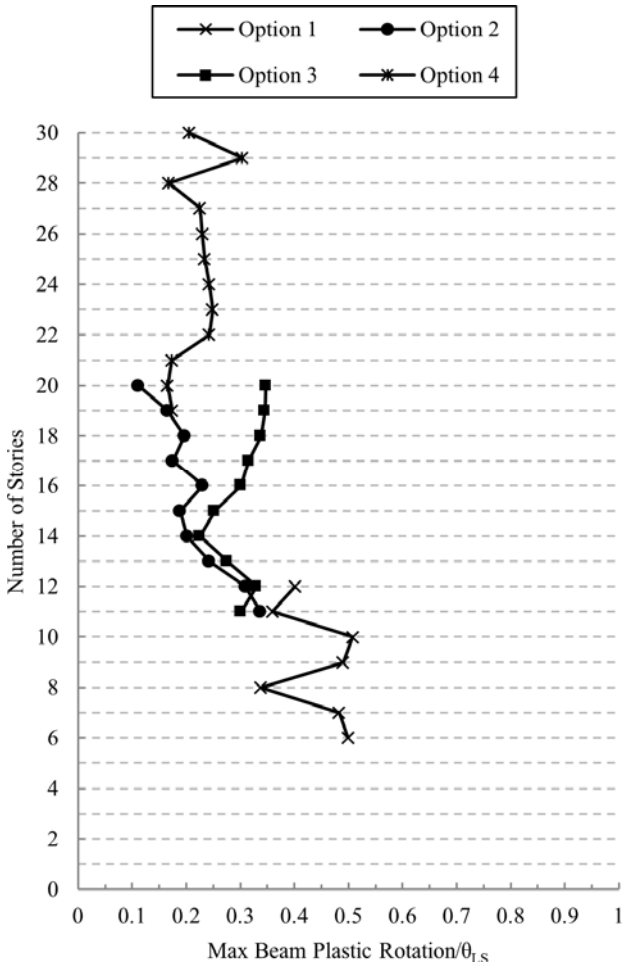

Figure 13: *Steel beam plastic rotation results and performance criteria*

2.4.4 BASE SHEAR

Also relevant for this study was the maximum base shear experienced by the structures under seismic excitation. Because the models were fixed at their base, they were essentially rigid in shear. Thus, for the design of this type of structure, it would be necessary to know the base shear demands so the foundation and base connections could be properly designed.

The mean of the maximum base shears averaged over all four options and the suite of ground motions is illustrated in Figure 14. Also plotted is the base shear predicted by the NBCC for several R factors ($R = R_dR_o$) based on the same 2% in 50 year spectrum shown in Figure 9. The design R factor (3) is highlighted with the thicker, solid line.

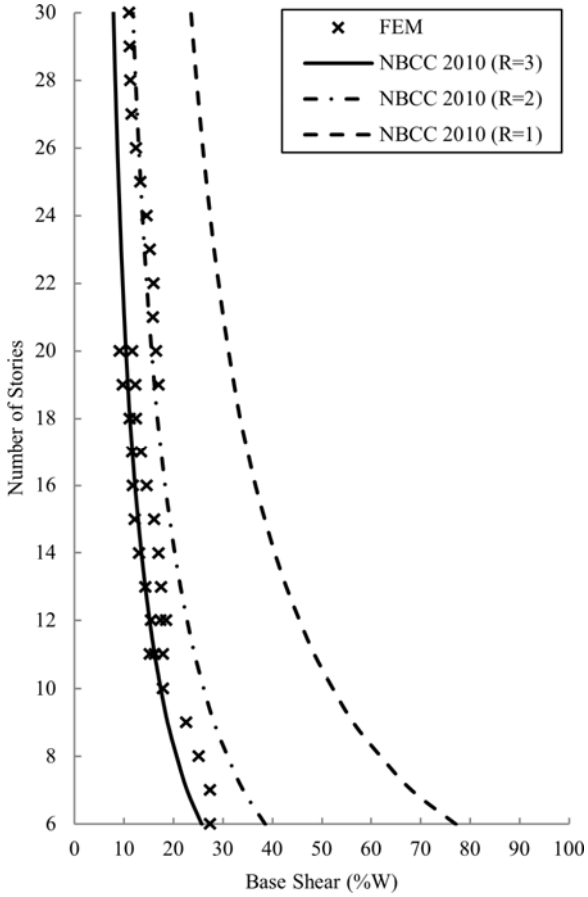

Figure 14: *Base shear results from FEMs compared to those predicted by NBCC 2010 for different R (R_dR_o) values*

3 DISCUSSION

From the results presented herein, it appears that the FFTT systems, as they were designed for this study, meet the performance required under design seismic loading. Interstorey drifts were lower than required and local plastic deformations were within a reasonable range for life safety performance.

The computed base shears correlated well with predictions based on the NBCC for the design R factors (=1.5). Moderately higher than predicted base shears were observed in the taller Option 4 models, that match more closely to the R_dR_o = 2 predictions. This could be for several reasons including higher mode effects increasing the base shear force in the structure more than anticipated. Also the taller models had stiffer LFRSs comprising many thick shear walls which induce large base reactions.

Maximum drifts and plastic deformations tended to decrease as the height of the structures was increased, as the taller, more flexible structures were less impacted by the seismic excitations. However, these characteristics, which made the taller structures less susceptible to damage induced by ground shaking, may cause serviceability issues under high wind loads. Additional studies are currently being conducted to assess this issue.

4 REFERENCES

[1] Green MC, Karsh JE (2012) TALL WOOD - The case for tall wood buildings. Vancouver: Wood Enterprise Coalition.

[2] Wilson, E., and Habibullah, A. Sap 2000 Integrated Finite Element Analysis and Design of Structures Basic Analysis Reference Manual. *Computers and Structures, Berkeley*, 1998.

[3] McKenna, F., Fenves, G. L., Scott, M. H., and Jeremic, B. Open System for Earthquake Engineering Simulation (OpenSees). Pacific Earthquake Engineering Research Center, University of California, Berkeley, CA, 2000.

[4] Gagnon, S and Pirvu, C. (Eds). CLT handbook: cross-laminated timber. FPInnovations, 2011.

[5] Blass, H. J., and Fellmoser, P. Design of solid wood panels with cross layers. *8th World Conference on Timber Engineering*. Vol. 14. No. 17.6, 2004.

[6] Buchanan, A. H., and Fairweather, R. H. Seismic design of glulam structures. *Bulletin of the New Zealand national society for earthquake engineering*, 26(4):415-436, 1993.

[7] Popovski, M., Schneider, J., and Schweinsteiger, M. Lateral load resistance of cross-laminated wood panels. *World Conference on Timber Engineering*, 20-24, 2010.

[8] CSA O86-09 Engineering design in wood. Canadian Standards Association, 2009.

[9] CSA S16-09 Handbook of Steel Construction. Canadian Institute of Steel Construction, 2009.

[10] Cross Laminated Timber Design Guide. Structurlam. 2014.

[11] Blass, H. J., and Görlacher, R. Rolling shear in structural bonded timber elements. *International conference on wood and wood fiber composites, Universität Stuttgart, Stuttgart*, 2000.

[12] Stürzenbecher, R., Hofstetter, K., and Eberhardsteiner, J. Cross laminated timber: a multi-layer, shear compliant plate and its mechanical behavior. *Proceedings of the World Conference on Timber Engineering*, 2010.

[13] Bhat, P. Experimental investigation of connection for the FFTT timber-steel hybrid system. MASc thesis, University of British Columbia, Vancouver, Canada, 2013.

[14] Ibarra, L F., and H Krawinkler. Global collapse of frame structures under seismic excitations. Pacific Earthquake Engineering Research Center, 2005.

[15] National Building Code of Canada. National Research Council Canada, 2010.

[16] Pei, S., Popovski, M., van de Lindt, J. W. Analytical study on seismic force modification factors for cross-laminated timber buildings. *Can. J. Civ. Eng.* 40:887-896, 2013.

[17] Hall, J. F. Problems encountered from the use (or misuse) of Rayleigh damping. *Earthquake engineering & structural dynamics*, *35*(5):525-545, 2006.

[18] Quantification of Building Seismic Performance Factors. FEMA-P695, 2009.

[19] ASCE/SEI 07-13 Minimum Design Loads for Buildings and Other Structures. American Society of Civil Engineers, 2013.

[20] Deierlein, G. G., Reinhorn, A. M., and Willford, M. R. Nonlinear structural analysis for seismic design. *NEHRP Seismic Design Technical Brief No. 4*, 2010.

[21] Mayes, R. L. Interstorey drift design and damage control issues. *The Structural Design of Tall Buildings*, 4(1):15-25, 1995.

[22] Development of Next Generation Performance-Based Seismic Design Procedures for New and Existing Buildings. FEMA-P58-1, 2012.

[23] ASCE/SEI 41-06 Seismic Rehabilitation of Existing Buildings. American Society of Civil Engineers, 2013.